Pak. J. Bot., 46(6): 2227-2238, 2014.

THE RELATIONSHIP BETWEEN FIBER INITIATION AND LINT PERCENTAGE IN COTTON

GUO XIAN[1†], MA JUN[1†], GUO YUPING[1], SUN MIZHEN[1], ZHOUJIAJIA[1], YUAN YANCHAO[1], ZHANG TIANZHEN[2], SUN XUEZHEN[1*] AND SONG XIANLIANG[1*]

[1]College of Agronomy/National Key Laboratory of Crop Biology, Shandong Agricultural University, Tai'an 271018, China;
[2]State Key Laboratory of Crop Genetics and Germplasm Enhancement, Cotton Research Institute, Nanjing Agricultural University, Nanjing 210095, China
[*]Corresponding authors e-mail: sunxz@sdau.edu.cn; songxl999@163.com.

Abstract

In this study, cytological observation of cotton fiber initiation from 1 d before anthesis to 3 d post anthesis (dpa) was performed using a scanning electron microscope. Six cotton chromosome segment introgression lines and their recipient/donor parents were used as materials. Results showed that fiber cell protrusions were highly related to genotype and germplasm, but fiber cell elongations were closely related to lint percentage. Fiber cell protrusions and elongations initially formed on the funicular crest, extended to the chalaza cap and the middle part of the ovule, and finally reached the micropyle. Fiber protrusion density at 1 dpa and elongation density at 2 dpa were observed in the following parts from highest to lowest: funicular crest > chalaza cap > middle part of the ovule > micropyle. The fiber protrusion density at 1 dpa and the fiber elongation density at 2 dpa were positively correlated with lint percentage and lint index but negatively correlated with seed index. The results of gray relational analysis were consistent with the correlation analysis results. Early fiber elongation contributed positively to protrusion density and elongation density, thereby resulting in a high lint percentage.

Key words: Lint percentage; Fiber initiation; Cytological observation; SEM; CSILs; Cotton.

Abbreviation: CSILs (chromosome segment introgression lines), ILs (introgression lines), dpa (days post anthesis), SEM (scanning electron microscopy), PBS (phosphate buffer solution)

Introduction

Cotton (*Gossypium* species) is one of the most important economical crops worldwide. Cotton fiber can be used to manufacture cotton yarn and cotton fabric. Cytological observations have been conducted to understand the fiber development of cotton lint fibers. Cotton fiber development is divided in four overlapping stages: fiber initiation stage; fiber elongation stage; secondary wall thickening stage; and maturation stage (Wilkins & Jernstedt, 1999; Willison & Brown, 1977; Li *et al*., 2009). Fiber initiation occurs at 1 d before anthesis (–1 dpa) (Ramsey & Berlin, 1976; Yang *et al*., 1999). Differentiation begins at the chalaza end of the ovule and then progresses to the micropylar end (Lang, 1938; Stewart, 1975). At 1 and 2 d postanthesis (dpa), spherical fiber initials begin to expand lengthwise, bending and growing toward the micropyle; at 3 dpa, these fibers clump together because they are sufficiently long and their tips taper (Stewart, 1975). Afterward, the fiber elongation ratio of fertilized ovules increases gradually (Van't Hof & Saha, 1998). At 15 dpa, this ratio reaches the maximum (Schubert *et al*., 1973) and then rapidly decreases at 20 dpa. The duration of the elongation stage lasts for 24 to 34 d, but this duration may be sensitively affected by the environment (Quisenberry & Kohel, 1975). Afterward, the secondary cell wall deposition begins (Hutchinson *et al*., 1947). At 50 dpa, the seeds of most of the cotton cultivars have dehisced and matured.

Cultivated cotton species are classified as two types of fibers: "lint" and "fuzz" (Lang, 1938; Hutchinson *et al*., 1947; Stephens, 1958; Fryxell, 1963 and 1964). Lint fiber is longer and easier to detach; this type of fiber is also the source of commercial cotton and the major part of fiber weight (Vollesen, 1987; Fryxell, 1992). Fuzz fiber is quite short and attaches to the seed during spin ginning (Stewart, 1975). Lint fiber appears on the day of anthesis, whereas fuzz fiber reportedly forms at 5 dpa to 9 dpa in *G. hirsutum* L. and at 12 dpa in *G. barbadense* L.; furthermore, fuzz fiber only forms in certain regions of the seed depending on species and/or variety (Lang, 1938; Joshi *et al*., 1967; Berlin, 1986).

The ratio and the amount of lint and fuzz contribute largely to lint percentage and lint index. Lint percentage, which is one of the three main factors affecting cotton fiber yield, is the ratio of the fiber weight to the total seed cotton weight of a plant. Initiation development and differentiation of cotton fiber are highly related to lint percentage and lint index. Several studies have reported about fiber initiation development patterns affecting variation in lint percentages, but most of these studies have focused on *G. hirsutum* intraspecies (Zhang *et al*., 2007; Butterworth *et al*., 2009; Li *et al*., 2009). However, genetic background interference is difficult to exclude.

† These authors contributed equally to this work.

This study described the fiber cell initiation patterns and the morphological changes in a series of cotton chromosome segment introgression lines (CSILs) developed by interspecific crossing, high-backcrossing, and selfing with marker-assisted selection approaches (Wang *et al*., 2008 and 2012). CSILs are single introgressed segments with pure genetic background and genetic stability compared with other materials (Guo *et al*., 2013). In our design, a series of CSILs was selected based on their evaluated traits and their recipient/donor parents. CSILs were then used to investigate fiber cell initiation to elucidate the essential mechanism among CSILs materials. These materials were also used to understand the similarities and differences between high and low lint percentage phenotypes with regard to fiber initiation and differentiation phases. This study may help elucidate the molecular mechanism of high and low lint percentage performances and provide a theoretical basis for the differentiation and development of cotton fiber.

Materials and Methods

Material planting: The materials used in this study were *G*. *hirsutum* L. cv. TM-1 (background parent of CSILs), *G*. *barbadense* L. cv. Hai7124 (donor parent of CSILs), three high lint percentage CSILs, and three low lint percentage CSILs identified based on a previous trait evaluation method in 2009 and 2010. The information of six selected CSILs is presented in Table 1. This set of CSILs was provided by the Cotton Research Institute, Nanjing Agricultural University, Nanjing, China. The detailed information about development and genotypic constitution of CSILs is provided by Wang *et al*., (2008; 2012). All of the materials were planted in Dezhou City, Shandong Province (in the Yellow River Basin cotton-growing areas), China in 2011 under normal field management conditions. Each material was planted in five rows that measured 10.0 m each.

Trait evaluation: In October 2011, 30 fully opened inner bolls on the first or the second fruiting branch in each row were collected to determine the traits. Seed cotton was placed in mesh bags, dried, and ginned using a roller ginning machine (SY-80, Linqing, Shandong province, China). Lint percentage (%), lint index (g), and seed index (g) were determined thrice as replicates. Lint percentage was determined as the ratio of the fiber weight to the seed weight. Seed index was measured as the weight of 100 ginned cotton seeds. Lint index was calculated using the following equation:

Lint index = lint percentage × seed index / (1 – lint percentage) (Zhang, 2004).

Significant difference was analyzed in SAS 8.0 (SAS Institute Inc., Cary, North Carolina, USA).

Cytological observation and data analysis: The flowers were tagged at –1 dpa or during the cotton flowering period on August 3 in 2011. Fresh immature ovaries were collected from –1 dpa to 3 dpa at 9:00 AM daily and placed in an ice box. At each stage, 20 to 30 ovules were stripped, fixed in 0.2 M phosphate buffer solution (PBS, pH = 7.4) with 3% glutaraldehyde for 2 h at 0°C to 4°C, and rinsed five times with PBS (0.2 M, pH = 7.4) for 15 min each. Afterward, the ovules were postfixed in H_2OsO_4 for 5 h and rinsed five times in PBS (0.2 M, pH = 7.4) for 15 min each. The ovules were then washed with ethanol in a series of 45%, 50%, 70%, 85%, and 95% for 30 min each. Afterward, the ovules were further washed with 100% ethanol for 3 hrs and then with tertiary butyl alcohol for 3.5 hrs. The materials were freeze dried and sputter coated with conductive gold paint. Afterward, these materials were observed and photographed using SEM (JSM-6610LV, Hitachi, Japan) at an accelerating voltage of 15 kV.

The photographs (magnification 500×) were captured from four positions of the ovule at various developmental stages (the funicular crest, the chalaza cap, the middle ovule, and one quarter of the ovular surface near the micropyle); three replicates were then generated. Protrusions at 1 dpa and elongations at 2 dpa in each region of the ovule were counted from the photographs.

Protrusion and elongation densities were calculated using the following equation:

$$FD \text{ (No. mm}^{-2}) = (X/Y) \times (M/N)^2$$

where *FD* is the fiber protrusion/elongation density, *X* is the number of fiber cell protrusion/elongation, *Y* is the frame-rectangular area, *M* is the actual scale length, and *N* is the scale length. The mean densities of the four positions were calculated as the fiber density (X_0) of each sample.

Correlation analysis and gray relational analysis were conducted to elucidate the relationship between fiber protrusion or elongation density and lint percentage-related traits. Correlation coefficients were estimated using SPSS 17.0 (SPSS, Chicago, Illinois, USA). Gray relational analysis was conducted using DPS 7.05 and SPSS 17.0. X_0 was used as the reference sequence, whereas the other traits were used to compare sequences. Non-dimensional parameters were used to standardize the original data, and the relational coefficient was calculated as follows:

$$\zeta_{i(k)} = \frac{\min_i \min_k \left[X_{o(k)} - X_{i(k)}\right] + \rho \min_i \max_k \left[X_{o(k)} - X_{i(k)}\right]}{\left[X_{o(k)} - X_{i(k)}\right] + \rho \max_i \max_k \left[X_{o(k)} - X_{i(k)}\right]}$$

where ρ is the distinguishing coefficient (in this study, ρ = 0.5). The relational degree was calculated based on the equal-weighted $r_i = \frac{1}{n}\sum_{k=1}^{n} \zeta_{i(k)}$ (Li *et al*., 2009).

Results

Performances of lint percentage, lint index, and seed index: In 2011, lint percentage, lint index, and seed index of the materials showed significant differences (Table 2). The lint percentage and the lint index of IL-08-7 and IL-10-1 were significantly higher than those of the background parent TM-1. The lint percentage and the lint index of IL-16-2-1 were significantly lower than those of TM-1, but the seed index was significantly higher than that of TM-1.

Table 1. Information of six selected CSILs.

CSILs	Chromosome	Position (cM)	Segment length (cM)	Characteristic
IL-08-7	A8\D1	112.35\54.70	14.2\7.1	High lint percentage
IL-10-1	A10\D10	2.26\12.40	17.7\14.2	High lint percentage
IL-22-2	D13	56.88	14.2	High lint percentage
IL-06-1	A6	41.62	28.3	Low lint percentage
IL-23-4	A2\D9	76.34\103.61	28.3\10.6	Low lint percentage
IL-16-2-1	A5\A11\A13	62.34\16.85\49.91	7.1\14.2\17.7	Low lint percentage

Table 2. Significant analysis of lint percentage related traits.

Material	Lint percentage (%)	Lint index (g)	Seed index (g)
TM-1	31.214	4.830	10.654
Hai7124	33.234*	4.852	9.764
IL-08-7	39.564**	6.538**	9.995
IL-10-1	37.043**	5.514**	9.371*
IL-22-2	34.575*	4.833*	9.874*
IL-23-4	27.775**	4.515	11.739**
IL-06-1	26.585**	4.378	12.081**
IL-16-2-1	22.394**	3.615**	12.553**

**indicate significant different at $P < 0.01$ compare with TM-1

* indicate significant different at $P < 0.05$ compare with TM-1

Ovule morphology at –1 dpa: SEMs of the ovular surface at –1 dpa are presented in Fig. 1. The anatropous ovule contained numerous stomata particularly on the funicular crest and the chalaza cap, which did not contain subsidiary cells (Fig. 1: ⑧ and ⑨). On the funicular crest of the ovule, Hai7124 contained the highest number of stomata followed by TM-1, IL-08-7, and IL-06-1. IL-10-1 and IL-16-2-1 contained the lowest number of stomata. IL-22-2 and IL-23-4 did not contain any stomata. The stomata of Hai7124 were larger and more mature than those of other materials (Fig. 1: ① to ⑧).

The comparison results of the panels in the figures showed that the fiber cell protrusions were found only on the ovular surface of Hai7124, in which dotted fiber protrusions were observed (Fig. 1: ① and ⑨). By contrast, high-lint percentage ILs (IL-08-7, IL-10-1, and IL-22-2) and low-lint percentage ILs (IL-06-1, IL-23-4, and IL-16-2-1) were found only on scattered stomata on the ovular surface of TM-1 (Fig. 1: ② to ⑧). The result showed that different cultivars varied in terms of fiber growth patterns. Fiber cell protrusion was highly related to genotype and germplasm.

Fiber cell protrusion at 0 and 1 dpa: Fiber initials appeared initially on the funicular crest and then around the ovule. Fiber initiation at the apex of the chalaza cap began after the fiber initials appeared on the sides of the ovule (Fig. 2: ① to ④). The extreme end of the micropyle was the last area where the fiber initials developed. In this extreme end, new fiber initials appeared at 3 dpa to 4 dpa. The fiber cell protrusions of all of the samples during anthesis were small with dome and irregular shapes, but such protrusions were distinguishable from non-fibrous protrusions which were sparsely and unevenly distributed on the ovular surface. The protrusion density on the ovular surface was relatively higher than that on the funicular crest but lower on the chalaza cap and the middle part of the ovule. This protrusion density was almost not determined near the micropyle (Fig. 2: ① to ④). In different samples, the protrusion densities on the funicular crest of Hai7124, IL-08-7, and IL-10-1 were higher than those of TM-1, IL-22-2, IL-06-1, IL-23-4, and IL-16-2-1 (Fig. 2 ① to ⑧). Although fiber protrusion was found on IL-16-2-1, this protrusion was a sunken oblate protrusion. The development of these protrusions seemed abnormal, thereby resulting in a low lint percentage (Fig. 2 ⑧).

At 1 dpa, the fiber initials diametrically expanded above the epidermis and began to extend toward the micropyle (Fig. 3 ① to ⑦). The high-lint percentage IL-08-7, IL-10-1, and IL-22-2 (Fig. 3 ③ to ⑤) showed sparse and irregular fiber cell protrusions in the micropyle region, but TM-1 (Fig. 3 ①), Hai7124 (Fig. 3 ②),IL-06-1, IL-23-4, and IL-16-2-1 (Fig. 3 ⑥ to ⑧) almost exhibited no fiber cell protrusion in the micropyle region. The fiber cell protrusions appeared as spherical or short cylindrical protrusions on the funicular crest (Fig. 3 ⑨ and ⑩), suggesting that the elongation period began. In IL-08-7 and IL-10-1, fiber cell elongations were evident on the funicular crest (Fig. 3 ⑪ to ⑬), extending to the chalaza cap and the middle part of the ovule, thereby reaching the micropyle region. By contrast, Hai7124 (Fig. 3 ⑩), TM-1 (Fig. 3 ⑨), IL-06-1, IL-23-4, and IL-16-2-1 (Fig. 3 ⑮ to ⑰) did not show evidence of fiber elongation in the ovular surface particularly IL-16-2-1, in which the fiber cell protrusions on the ovular surface were relatively sparse (Fig. 3 ⑱). These findings showed that fiber cell elongation was highly related to lint percentage.

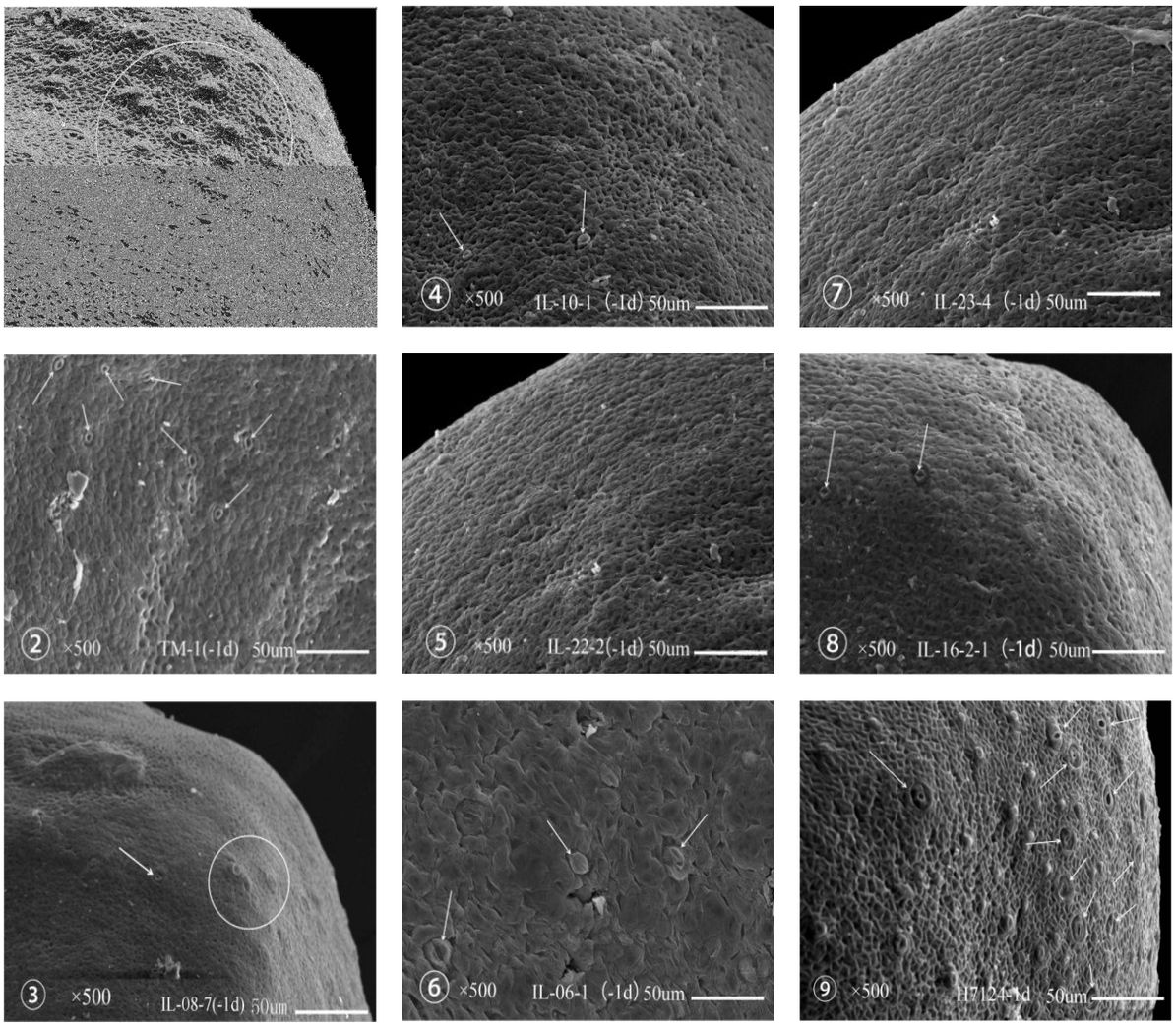

Note: Stomata are indicated with arrows and protrusions are in the circles.
Fig. 1. Scanning electron micrographs of ovule morphology at -1 dpa.

Fiber cell elongation at 2 and 3 dpa: At 2 dpa, most of the fiber cells exhibited evident elongations except the micropyle, where few spherical or hemispherical fiber cell protrusions were found (Fig. 4 ① to ⑧). At 2 dpa, the fibers of Hai7124 also began to adhere, aggregate in small groups, and form a spiral growth (Fig. 4 ⑨ and ⑩). The tips tapered (Fig. 4 ⑪). By contrast, the fibers of the other materials (Fig. 4 ⑫ to ⑱) at 2 dpa continued to grow independently without adhering to or segregating in small groups. Spiral growth and tapered fiber tips were also not evident (Fig. 4 ⑪).

Cotton fibers rapidly elongated and the morphology changed at 3 dpa. The cotton ovules of the samples were tightly packed with the rapidly elongated fiber (Fig. 5, ①). The fiber morphologies of different materials varied. In particular, the fiber lengths of the long staple cotton Hai7124 (Fig. 5 ③) and the high-lint percentage IL-08-7 (Fig. 5 ④) were longer than those of the background parent TM-1 (Fig. 5 ②). This result indicated the good characteristics of Hai7124 and IL-08-7. As growth continued, the fiber tips of the samples at 3 dpa tapered at a greater extent than those at 2 dpa, whereas the fibers of TM-1 and the six CSILs continued to grow independently. Spiral growth was not evident even on the ovular surface of Hai7124 (Fig. 5, ⑤ to ⑫).

Comparison between fiber protrusion density and elongation density on the ovular surface: The different materials were compared to determine the relationship between fiber density and fiber initial development of the different samples. The fiber density in the fiber protrusion period (at 1 dpa) was determined as the fiber protrusion density. The fiber density during the fiber elongation period (at 2 dpa) was calculated as the fiber elongation density. The results showed that the highest fiber protrusion density and fiber elongation density of the samples were found on the funicular crest, followed by those on the chalaza cap and the middle part of the ovule. The micropyle exhibited the lowest density. The fiber densities on these four positions exhibited significant differences (Table 4).

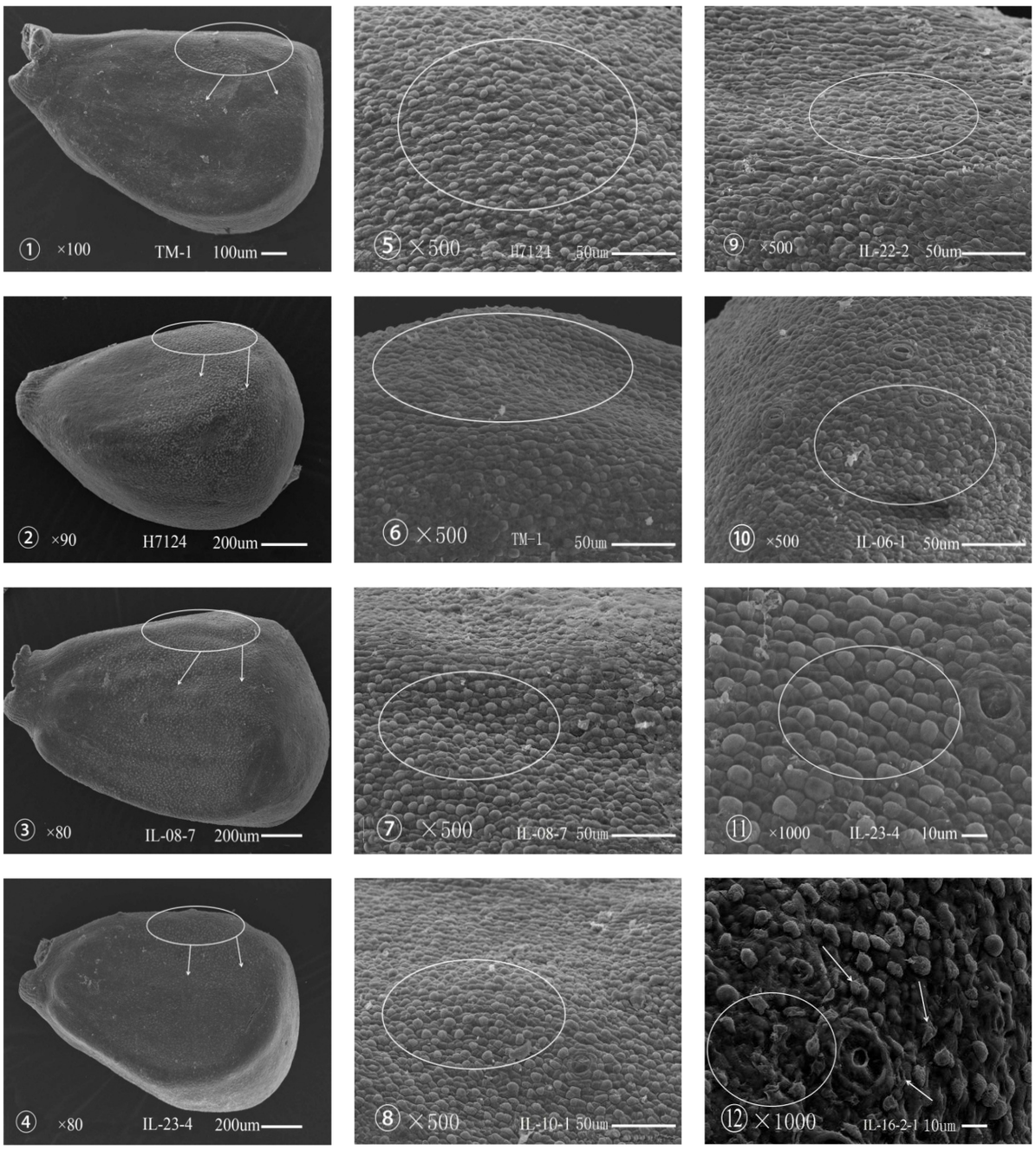

Note: Arrows indicate the direction of protrusion initial on the ovule surface and protrusion densities of various materials are encircled.
Fig. 2. Scanning electron micrographs of fiber cell protrusion on the day of anthesis (0 dpa).

The average fiber densities at 1 and 2 dpa of eight materials are listed in Table 5. At 1 dpa, the highest fiber protrusion density (7533/ mm^2) was observed in Hai7124 (lint percentage = 33.234%). The high-lint percentage IL-08-7 (39.564%, 6888/mm^2), IL-10-1 (37.043%, 6732/mm^2), and IL-06-1 (26.585%, 4777/mm^2) also showed high fiber protrusion densities. TM-1 (31.214%, 4635/mm^2), IL-22-2 (30.575%, 4378/mm^2), and IL-23-4 (27.775%, 4217/mm^2) exhibited relatively high protrusion densities. The lowest fiber protrusion density and lint percentage were observed in IL-16-2-1 (22.394%, 4062/mm^2). At 2 dpa, the highest fiber elongation density was observed in IL-08-7 (39.564%, 4647/mm^2) followed by IL-10-1 (37.043%, 4582/mm^2), IL-06-1 (26.585%, 4105/mm^2), IL-22-2 (30.575%, 4036/mm^2), TM-1 (31.214%, 4011/mm^2), and IL-23-4 (27.775%, 3907/mm^2). The lowest lint percentage was observed in IL-16-2-1 (22.394%, 3580/mm^2). These results showed that the fiber densities of IL-08-7 and IL-10-1 were significantly higher than those of TM-1. By contrast, the fiber densities of IL-06-1, IL-23-4, and IL-16-2-1 were significantly lower than those of TM-1.

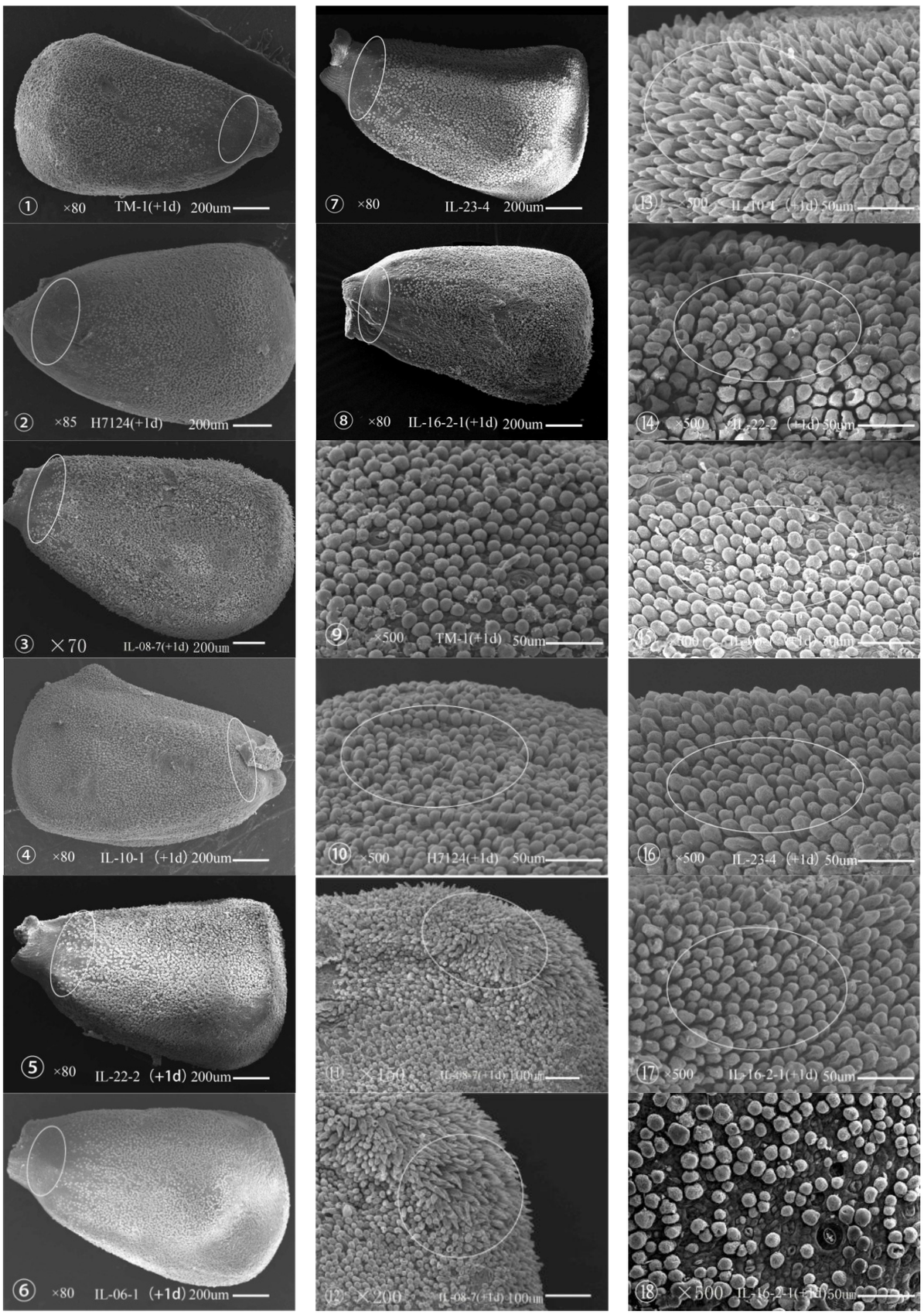

Fig. 3. Scanning electron micrographs of protrusion at 1 dpa.

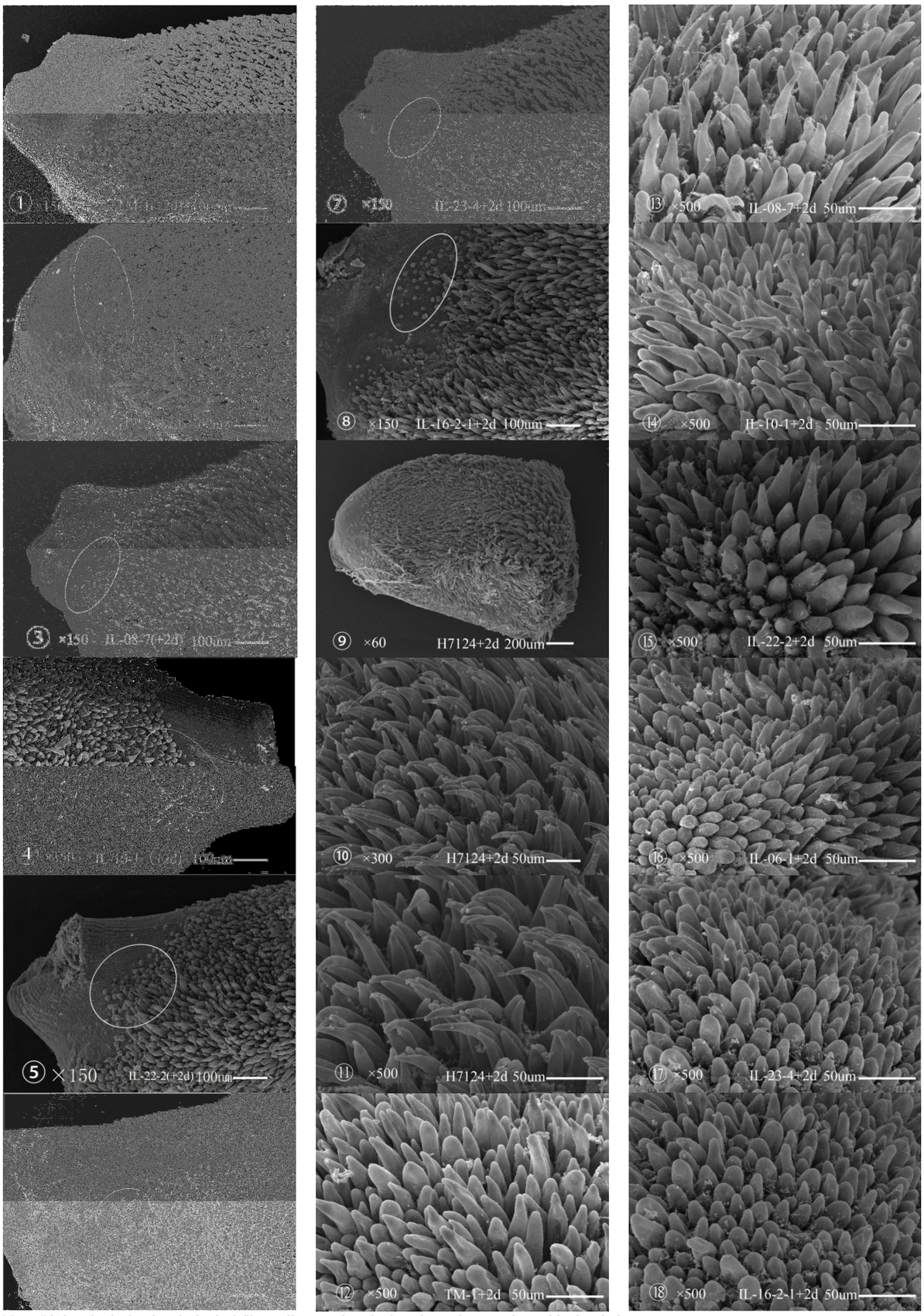

Note: Little spherical or hemispherical fiber cell protrusions in the micropyle were showed in the circles.
Fig. 4. Scanning electron micrographs of elongation at 2 dpa.

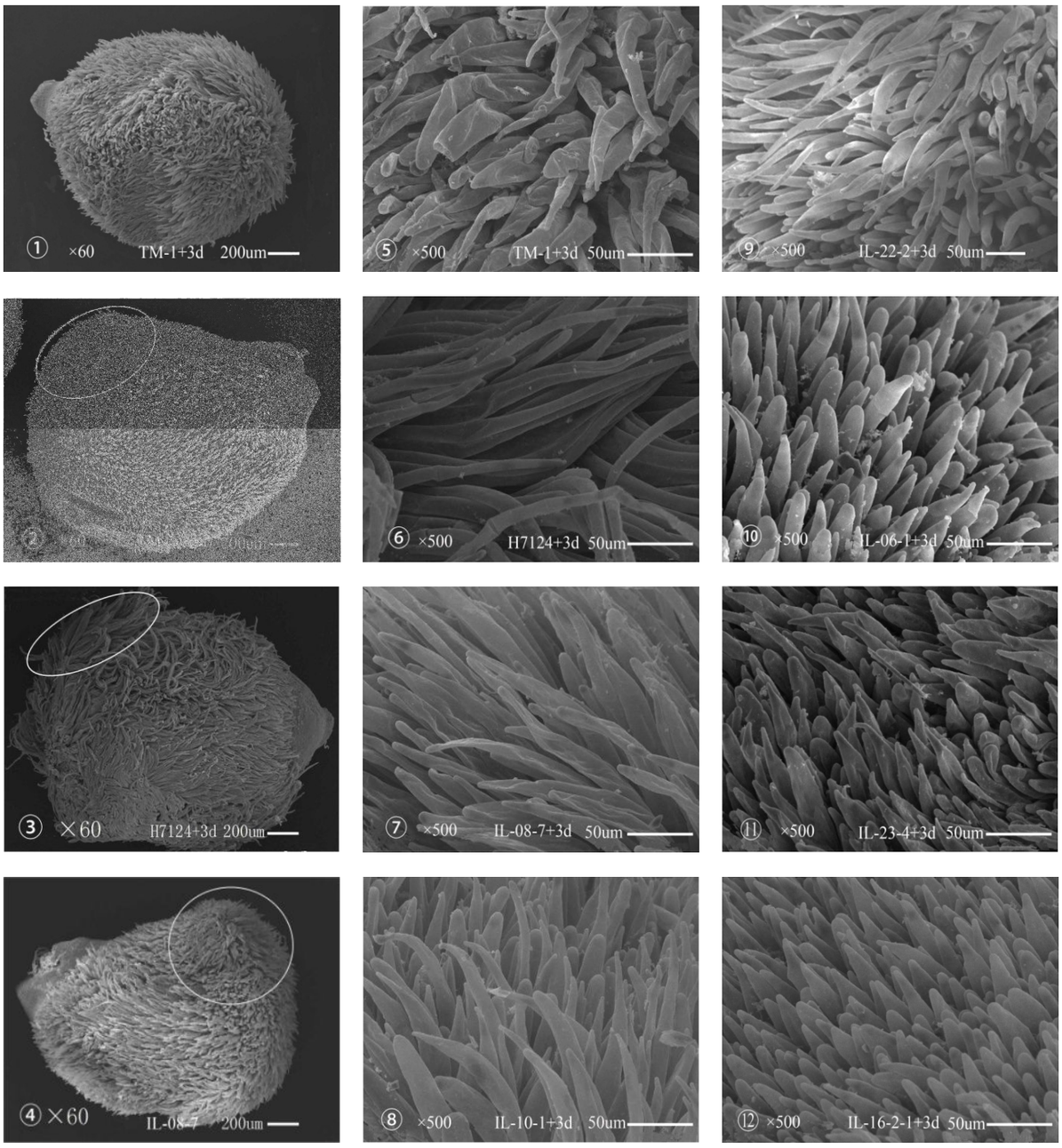

Note: Fiber density comparisons are showed in the circles.
Fig. 5. Scanning electron micrographs of elongation at 2 dpa.

"Protrusion density-elongation density" and "protrusion density/elongation density" (Table 5) indicated the degree of fiber elongation and the decrease in fiber density on the ovular surfaces from 1 dpa to 2 dpa. Hai7124 showed the highest protrusion density-elongation density and protrusion density/elongation density (33.234%, 3783, 2.01). IL-08-7 (39.564%, 2242, 1.48), IL-10-1 (37.043%, 2150, 1.47), IL-06-1 (26.585%, 672, 1.16), TM-1 (31.214%, 625, 1.16), IL-16-2-1 (22.394%, 482, 1.13), and IL-22-2 (30.575%, 342, 1.08) also exhibited high protrusion density-elongation density and protrusion density/elongation density. The lowest protrusion density-elongation density and protrusion density/elongation density were observed in IL-23-4 (27.775%, 309, 1.08). Furthermore, protrusion density-elongation density and protrusion density/elongation density of IL-08-7 and IL-10-1 were significantly higher than those of the background parent TM-1. By contrast, the protrusion density-elongation density and protrusion density/elongation density of IL-06-1, IL-23-4, and IL-16-2-1 were significantly lower than those of TM-1.

Correlation and gray relation analyses between fiber density and lint percentage-related traits: Correlation and gray relational analyses of fiber protrusion/elongation density and lint percentage-related traits were conducted to quantify the relationship between these two factors (Table 3).

Table 3. Correlation coefficients and grey relational degrees between fiber density and fiber-related traits.

Fiber density	Lint percentage	Lint index	Seed index
Fiber protrusion density	0.816*/0.729	0.744*/0.689	-0.751*/0.461
Fiber elongation density	0.860**/0.732	0.887**/0.773	-0.645/0.653

Note: Correlation coefficient/Grey relational degree

* Denote significant correlation at $p \leq 0.05$; ** Denote significant correlation at $p \leq 0.01$

Table 4. Comparison of fiber density at 1 and 2 dpa among four positions of eight materials (x ±SD, No. mm^{-2}).

Material	Fiber protrusion density at 1 dpa				Fiber elongation density at 2 dpa			
	FC	CC	MPO	QNM	FC	CC	MPO	QNM
TM-1	6822±59Aa	6461±29Bb	3580±81Cc	1678±18Dd	4384±65Aa	4069±6Bb	3919±24Cb	3672±18Dc
Hai7124	11648±104Aa	10091±94Bb	5137±47Cc	3255±47Dd	4593±21Aa	4020±37Bb	3375±25Cc	3009±14Dd
IL-08-7	8238±45Aa	6820±56Bb	6366±58Cc	6128±58Dc	5452±12Aa	5147±47Bb	4038±18Cc	3950±25Dc
IL-06-1	6714±24Aa	5227±58Bb	4937±54Cc	2228±20Dd	4551±23Aa	4112±18Ba	4358±19Cb	3398±59Dc
IL-10-1	8545±29Aa	7894±87Bb	5656±70Cc	4832±26Dd	5398±38Aa	4979±38Bb	4030±23Cc	3921±20Dc
IL-22-2	5737±42Aa	4333±65Bb	3818±64Cc	3623±59Dc	4464±68Aa	4270±34Ba	3769±20Cb	3641±30Cb
IL-23-4	4893±76Aa	4721±16Aa	3845±70Bb	3408±88Cc	4198±37Aa	3988±36Bb	3805±58Cb	3638±25Dc
IL-16-2-1	4568±68Aa	4564±50Aa	3662±58Bb	3453±20Cb	3747±26Aa	3975±53Bb	3630±46Bb	2969±17Cc

In the same line, the letters "A, B, C, D" denote significant difference at $p<0.05$; the letters "a, b, c, d" denote highly significant difference at $p<0.01$

FC: Funicular crest; CC: Chalazal cap; MPO: Middle part of ovule; QNM: One quarter of ovular surface near micropyle

Table 5. Comparison between average fiber density of eight cotton materials.

Material	Fiber protrusion density	Fiber elongation density	Fiber protrusion density/ Fiber elongation density	Fiber protrusion density/ Fiber elongation density
TM-1	4635 ± 7Ee	4011 ± 23Dc	625 ±19Dc	1.16
Hai7124	7533 ± 6Aa	3749 ± 7Fe	3783 ± 11Aa	2.01
IL-08-7	6888 ± 23Bb	4647 ± 20Aa	2242 ± 41Bb	1.48
IL-06-1	4777 ± 7Dd	4105 ± 5Cb	672 ± 12Dc	1.16
IL-10-1	6732 ± 19Cc	4582 ± 23Ba	2150 ± 35Cb	1.47
IL-22-2	4378 ± 21Ff	4036 ± 24Db	342 ± 38Fe	1.08
IL-23-4	4217 ± 28Gg	3907 ± 13Ed	309 ± 40Fe	1.08
IL-16-2-1	4062 ± 18Hh	3580 ± 16Gf	482 ± 29Ed	1.13

In the same line, the letters "A, B, C, D, E, F, G, H" denote significant difference at $p<0.05$; the letters "a, b, c, d, e, f, g, h" denote highly significant difference at $p<0.01$

The correlation analysis result showed that the fiber protrusion density at 1 dpa was positively correlated with the lint percentage and the lint index but negatively correlated with the seed index. The correlation coefficients of the following factors were arranged from highest to lowest: lint percentage (0.816) > lint index (0.744) > seed index (–0.751).

The gray relational degree between the fiber protrusion density and other factors was arranged from highest to lowest: lint percentage (maximum of 0.729) > lint index (0.689) > seed index (0.461). This result was consistent with the correlation analysis result.

Likewise, fiber elongation density was positively correlated with lint index and lint percentage but negatively correlated with seed index. The correlation coefficients of the following factors were arranged from highest to lowest: lint index (maximum of 0.887) > lint percentage (0.860) > seed index (–0.645). Gray relational analysis result suggested that the relational degree between fiber elongation density and other factors was arranged from highest to lowest: lint index (0.773) > lint percentage (0.732) > seed index (0.653). These two analyses exhibited a slight distinction, but the close correlation between elongation density and lint percentage-related traits was consistent.

Discussion

Stomata on the ovular surface: Joshi *et al*., (1967) and Stewart (1975) discussed the formation of stomata on cotton ovules. Stomata appear on the chalaza end of the ovule at –1 or –2 dpa and subsequently differentiate on the entire surface. However, Stewart (1975) indicated that few stomata appear on the ovule surface at least one week before anthesis, and numerous stomata develop on the chalaza end as anthesis begins. The mature stomata

are of anomocytic type with two guard cells but no subsidiary cells. In the current study, the presence of stomata was observed on the ovular surface at –1 dpa. Numerous stomata without subsidiary cells were found in the anatropous ovule specifically on the funicular crest and the chalaza cap; this finding is consistent with previous observations (Stewart, 1975; Joshi *et al*., 1967). Furthermore, the number and the size of the stomata varied among the different samples. The stomata of Hai7124 were higher in number and larger in size than those of the other seven materials. This result indicated that the number and the size of stomata may be related to genotype and affect fiber initiation. To clarify this assumption, we recommend that further studies should be conducted.

Time sequence of fiber initiation on the ovular surface: Considering the time sequence of fiber initiation on the ovular surface, Lang (1938) reported that fiber initials form initially on the chalaza of the ovule at anthesis and new initials sequentially develop toward the micropylar end after anthesis. Joshi *et al*., (1967) also reported similar observations. By contrast, Stewart (1975) demonstrated that fiber initials appear initially on the funicular crest and spread around the lateral circumference of the ovule; the formation of fiber initials on the chalaza cap is delayed for a few hours; this formation is further delayed for 3 d to 4 d on the chalaza cap and the extreme end of the micropylar region. Stewart's findings were confirmed by other studies (Xu *et al*., 1987; Dong *et al*., 1989; Applequist *et al*., 2001; Zhang *et al*., 2007; Li *et al*., 2007 and 2009). In our study, fiber initiation and differentiation from 1 dpa to 3 dpa showed that the fiber initials and the elongated fibers developed initially on the funicular crest and subsequently formed on the chalaza cap, the middle part of the ovule, and the micropyle, where the formation of the fiber initials was delayed until 3 dpa to 4 dpa. The observation regarding the time sequence of fiber initiation on the ovular surface strongly supported previous findings (Stewart, 1975).

Morphological change in fiber initiation: The early development of fibers comprises two overlapping steps designated as (1) spherical expansion above the epidermis and (2) elongation (Stewart, 1975). Cotton seed trichomes expand via a diffused growth (Tiwari & Wilkins, 1995). In the current study, the spherical expansion of the samples began at anthesis and lasted for about 2 d except Hai7124, in which dotted fiber protrusion began at –1 dpa. At 0 dpa, the fiber cell protrusions in the samples were small with dome and irregular shapes, but such protrusions were distinct from the non-fibrous protrusions. At 1 dpa, the fiber initials diametrically expanded above the epidermis and extended toward the micropyle, where only IL-08-7, IL-10-1, and IL-22-2 contained sparse and irregular fiber cell protrusions. The fiber cell protrusions of the samples were spherical or short cylindrical on the funicular crest, suggesting that these protrusions possibly entered the elongation period. Fiber cell elongation was evident in IL-08-7 and IL-10-1. By contrast, fiber elongation was not observed on the ovular surfaces of the other materials. At 2 dpa, fiber cell elongations of the samples became more evident on the ovular surface except on the micropyle, where only few spherical or hemispherical fiber cell protrusions were found. The fiber initials of Hai7124 began to adhere, aggregate in small groups, and exhibit a spiral growth with tapered fiber tips. By contrast, the fibers of the other materials continued to grow independently and the fiber tips remained blunt. At 3 dpa, the cotton ovules of the samples were tightly packed by the rapidly elongated fiber, and the fiber morphologies of different materials varied. The fiber tips of the samples tapered to a larger extent at 3 dpa than at 2 dpa as growth continued.

Fiber density: All of the epidermal cells on the ovular surface became primordial fibers except the stomata and the micropylar cells; however, not all of these cells can differentiate to form fibers (Beasley, 1975; Berlin, 1986). The fiber density and the surface area of the seed affect the total number of fibers of a seed (Stewart, 1975). The ratio of differentiating cells to the total number of epidermal cells is approximately 1.0 to 3.7, and the density of fiber initials is approximately 3300 per mm^2 of the ovular surface. Approximately 15% to 25% of the cells differentiate to form lint fibers (Basra & Malik, 1984; Wilkins & Jernstedt, 1999).To quantify and elucidate the relationship between fiber density and fiber initials, we determined the fiber protrusion density and the fiber elongation density at 1 and 2 dpa, respectively. The results showed that the fiber protrusion density and the fiber elongation density of the samples were found in the following parts from highest to lowest: funicular crest > chalaza cap > middle part of the ovule > micropyle. In addition, the fiber elongation densities of the materials at 2 dpa were significantly lower than those at 1 dpa, indicating that the degree of fiber elongation and the decrease in fiber density on the ovular surfaces caused by the increase in the ovular volume of cotton may be related to lint percentage from 1 dpa to 2 dpa. This result is consistent with that in previous studies (Li *et al*., 2007 and 2009; Zhang *et al*., 2007).

Lint and Fuzz: Lint fiber initials of *G. hirsutum* are present in the spherical expansion phase at anthesis (Beasley, 1975; Stewart, 1975), whereas fuzz fibers are formed at 5 dpa to 9 dpa in *G. hirsutum* L. and only present in certain regions of the seed depending on species and/or variety (Lang, 1938; Joshi *et al*., 1967; Beasley, 1975). Lint and fuzz fiber bases are structurally similar but with minor differences. For example, the epidermal embedded "foot" of lint fibers is broader than that of fuzz fibers; lint fibers are detached at the elbow (Fryxell, 1963 and 1964). Fuzz protrusion projections do not resemble bubbles; instead, these projections are cylindrical with inadequate turgor pressure to elongate and reach the same length of lint fibers (Zhang *et al*., 2007).

In the present study, the fiber initials from –1 dpa to 3 dpa were observed in two different cultivars of TM-1, Hai7124, and a series of CSILs. However, a broader sampling of taxa and a longer developmental time frame were required to elucidate the origin of fuzz fibers. For example, the study period could be extended to 10 dpa

because fiber initials would be formed at this time. In addition, diploid and tetraploid cotton cultivars should be included because cultivars may exhibit different growth patterns (Quisenberry & Kohel, 1975).

Potential mechanisms of fiber development in different IL materials: Previous studies showed that the developmental morphology of fiber initiation is well characterized in upland cotton, but the morphology of sea-island cotton is rarely known, particularly the comparison between these two species. In the present study, a series of CSILs derived from a cross between the recipient parent *G. hirsutum* cv. TM-1 and the donor parent *G. barbadense* cv. Hai7124 was used. CSILs were single introgressed segments with pure genetic background and genetic stability compared with other materials. Six ILs contained single or a few introgressed segments from the donor parent Hai7124, and the rest of the chromosomal segments were similar to those of TM-1. These introgressed segments could result in morphological differences in fiber initiation and developmental stages among the materials.

At –1 dpa, Hai7124 contained the highest stomata on the funicular crest of the ovule, followed by TM-1, IL-08-7, and IL-06-1. However, no stomata were found on the funicular crest of the ovule in IL-22-2. During anthesis, IL-16-2-1 showed a sunken oblate protrusion on the funicular crest and differed from other materials. This observation suggested that the development of these protrusions may be abnormal and may not produce mature cotton fibers, thereby resulting in a low lint percentage. At 1 dpa, fiber cell elongations were initially evident on the funicular crest of IL-08-7 and IL-10-1. These elongations extended to the chalaza cap, the middle part of the ovule, and the micropyle. IL-22-2 did not show fiber elongation on the ovular surface. The fiber morphologies of different materials also varied at 2 dpa. The fiber length of IL-08-7 was longer than that of the background parent TM-1. The other two high-lint percentage materials (IL-10-1 and IL-22-2) did not exhibit significant fiber elongation.

We found that different materials exhibited various performances during the fiber development stage. Although IL-08-7, IL-10-1, and IL-22-2 showed high lint percentages in the final stages, their cytological morphologies varied. Differences were also found in low-lint percentage IL-23-4, IL-06-1, and IL-16-2-1. The results of our correlation and gray relation analyses showed that lint percentage was significantly related to fiber initiation. Various materials may exhibit different fiber initiation mechanisms during fiber development stages, thereby resulting in the final lint percentage performances. The genome of ILs only differed in small introgressed segments compared with those of TM-1. Considering this result, we deduced that different introgressed chromosome segments controlled fiber initiation mechanisms at different development stages**.** To verify this assumption, we will integrate these different introgressed chromosome segments in one material and observe the outcome in future studies.

Acknowledgements

We thank Yankui Guo (College of Life Science, Shandong Agricultural University, China) for his technical guidance for operation of SEM and Professor Tianzhen Zhang (Cotton Research Institute, Nanjing Agricultural University, China) for providing seed of CSILs.

This work was financially supported by grants from Shandong province System of Modern Agriculture Industrial Technology (Cotton industry), Science and Technology Development Project of Shandong province (2012GGB01026), Shandong Agricultural Breeding Project (2010LZ005, 2012LZcotton and cotton germplasm innovation of 2013) and Natural Science Foundation Project of Shandong Province (ZR2013CM005).

References

Applequist, W.L., R. Cronn and J.F. Wendel. 2001. Comparative development of fiber in wild and cultivated cotton. *Evol. & Dev*., 3: 3-17.

Basra, A.S. and C.P. Malik. 1984. Development of the cotton fiber. *Int. Rev. Cytol*., 89: 65-113.

Beasley, C.A. 1975. Developmental morphology of cotton flowers and seed as seen with the scanning electron microscope. *Am. J. Bot*., 62: 584-592.

Berlin, J.D. 1986. The outer epidermis of the cotton seed, cotton physiology. (Eds.): Mauney, J.R., Stewart, J.M. pp. 375-413.

Butterworth, J.M., J.R. Ellis, A.R. Raklev and G.P. Salam. 2009. Discovering baryon-number violating neutralino decays at the LHC. *Phys. Rev. Lett*., 103: 241803.

Dong, H.Z., C.N. Xu and B.S. Yu. 1989. A comparative study on cotton fiber development between upland cotton and sea-island cotton (I): cotton fiber differentiation. *Acta Agri. Univ. of Pekinensis*. 15: 377-381.

Fryxell, P.A. 1963. Morphology of the base of seed hairs of *Gossypium* I. Gross morphology. *Bot. Gazette*., 124: 196-199.

Fryxell, P.A. 1964. Morphology of the base of seed hair of *Gossypium* II. Comparative morphology. *Bot. Gazette*., 125: 108-118.

Fryxell, P.A. 1992. A revised taxonomic interpretation of *Gossypium* L. (Malvaceae). *Rheedea*., 2: 108-165.

Guo, X., Y.P. Guo, J. Ma, F. Wang, M.Z. Sun, L.J. Gui, J.J. Zhou, X.L. Song, X.Z. Sun and T.Z. Zhang. 2013. Mapping heterotic loci for yield and agronomic traits using chromosome segment introgression lines in cotton. *J. Integr. Plant Biol. Publish Online*. DOI:10.1111/jipb.12054.

Hutchinson, J.B., R.A. Silow and S.G. Stephens. 1947. The evolution of Gossypium and the differentiation of the cultivated cottons, pp: 160. London: Oxford University Press

Joshi, P.C., A.M. Wadhwani and B.M. Johri. 1967. Morphological and embryological studies of *Gossypium* L.. *Natl. Inst. of Sci. of India*, 33B: 37-93.

Li C.Q., W.Z. Guo and T.Z. Zhang. 2007. Comparative studies on fiber initiation development of four cultivated cotton species. *Acta Agronomica Sinca*., 33: 1346-1351.

Lang, A.G. 1938. The origin of lint and fuzz hairs of cotton. *J. Agr. Res*., 56: 507-521.

Li, C.Q., W.Z. Guo and T.Z. Zhang. 2009. Fiber initiation development in upland cotton (*Gossypium hirsutum* L.) cultivars with varied lint percentage. *Euphytica*, 165: 223-230.

Quisenberry, J.E. and R.J. Kohel. 1975. Growth and development of fiber and seed in upland cotton. *Crop Sci*., 15: 463-467.

Ramsey, J.C. and J.D. Berlin. 1976. Ultrastructure of early stages of cotton fiber differentiation. *Bot. Gazette*, 137: 11-19.

Schubert, A.M., C.R. Benedict, J.D. Berlin and R.J. Kohel. 1973. Cotton fiber development-kinetics of cell elongation and secondary wall thickening. *Crop Sci*., 13: 704-709.

Stephens, S.G. 1958. Factors affecting seed dispersal in Gossypium and their possible evolutionary significance. *N.C. Agr. Exp. Stn*., 131: 3-32.

Stewart, J.M. 1975. Fiber initiation on the cotton ovule (*Gossypium hirsutum* L.). *Am. J. Bot*., 62: 723-730.

Tiwari, S.C. and T.A. Wilkins. 1995. Cotton (*Gossypium hirsutum*) seed trichomes expand via diffuse growing mechanism. *Can. J. Bot*., 3: 746-757.

Van't Hof, J. and S. Saha. 1998. Growth and mitotic potential of multicelled fibers of cotton (Malvaceae). *Am. J. Bot*., 85: 25-29.

Vollesen, K. 1987. The native species of *Gossypium* (Malaceae) in Africa, Arabia and Pakistan. *Kew Bull*., 42: 337-349.

Wang, P., Y.J. Zhu, X.L. Song, Z.B. Cao, Y.Z. Ding, B.L. Liu, X.F. Zhu, S. Wang, W.Z. Guo and T.Z. Zhang. 2012. Inheritance of long staple fiber quality traits of *Gossypium barbadense* in *G. hirsutum* background using CSILs. *Theor. Appl. Genet*., 124: 1415-1428.

Wang, P., Y.Z. Ding, Q.X. Lu, W.Z. Guo and T.Z. Zhang. 2008. Development of *Gossypium barbadense* chromosome segment substitution lines in the genetic standard line TM-1 of *Gossypium hirsutum*. *Chinese Sci. Bull*., 53: 1065-1069.

Wilkins, T.A. and J.A. Jernstedt. 1999. Molecular genetics of developing cotton fibers, Cotton fibers. (Ed.): Basra, A.M., New York: Hawthorne Press, pp. 231-267.

Willison, J.H.M. and R.M. Brown. 1977. An examination of the developing cotton fiber: wall and plasmalemma. *Protoplasma*, 92: 21-41.

Xu, C.N., Y. Zhang, B.S. Yu, Q.W. Lin, Y.N. Xiao and J.Z. Jia. 1987. The comparative studies of early of fiber development of four cultivated cotton species with the scanning electron microscope. *Acta Agr. Univ. of Pekinensis*. 13: 255-262.

Yang, Y.M., J.Z. Jia, C.N. Xu, H.Y. Li and Y.H. Guo. 1999. Initiation of cotton fiber cells and the effects of temperature and plant growth substances on it. *J. China Agric. Univ*., 4: 15-22.

Zhang, D.Y., T.Z. Zhang, Z.Q. Sang and W.Z. Guo. 2007. Comparative development of lint and fuzz using different cotton fiber-specific developmental mutants in *Gossypium hirsutum*. *J. Integr. Plant Biol*. 49: 1038-1046.

Zhang, T.Z. 2004. Cotton Breeding, Crop breeding monograph. (Ed.): Gai, J.Y. Beijing: China Agriculture Press, pp. 415-454.

(Received for publication 20 July 2013)